

Article

Preparation and Self-Healing Application of Isocyanate Prepolymer Microcapsules

Guifeng Xiang [†], Jing Tu [†], Heng Xu, Jie Ji, Li Liang, Haozhe Li, Haoran Chen, Jingqing Tian and Xiaode Guo ^{*}

National Special Superfine Powder Engineering Technology Research Center of China, Nanjing University of Science and Technology, Nanjing 210094, China; xgfeng888@163.com (G.X.); tujing19960808@163.com (J.T.); xu_heng1995@163.com (H.X.); season18252588980@163.com (J.J.); xgfeng24@163.com (L.L.); 379152021lh@163.com (H.L.); xgf0911@163.com (H.C.); tjq112cn@163.com (J.T.)

^{*} Correspondence: guoxiaodeng@sina.com; Tel.: +86-137-0140-3693

[†] These authors contributed equally to this work.

Abstract: In this study, we successfully manufactured polyurethane microcapsules containing isocyanate prepolymer as a core material for self-healing protection coatings via interfacial polymerization of a commercial polyurethane curing agent (Bayer L-75) and 1,4-butanediol (BDO) as a chain extender in an emulsion solution. With an optical microscope (OM) and a scanning electron microscope (SEM), the resulting microcapsules showed a spherical shape and an ideal structure with a smooth surface. Fourier transform infrared spectra (FTIR) showed that the core material was successfully encapsulated. Thermal gravimetric analysis (TGA) showed that the initial evaporation temperature of the microcapsules was 270 °C. In addition, we examined the influence of the concentration of the emulsifier and chain extender on the structure and morphology of the microcapsules. The results indicate that the optimal parameters of the microcapsule are an emulsifier concentration of 7.5% and a chain extender concentration of 15.38%. Microcapsules were added to the epoxy resin coating to verify the coating's self-healing performance by a surface scratch test, and the results showed that the cracks could heal in 24 h. Furthermore, the self-healing coating had excellent corrosion resistance.

Keywords: microcapsules; isocyanate prepolymer; coating; self-healing



Citation: Xiang, G.; Tu, J.; Xu, H.; Ji, J.; Liang, L.; Li, H.; Chen, H.; Tian, J.; Guo, X. Preparation and Self-Healing Application of Isocyanate Prepolymer Microcapsules. *Coatings* **2022**, *12*, 166. <https://doi.org/10.3390/coatings12020166>

Academic Editor: Flavio Deflorian

Received: 23 December 2021

Accepted: 14 January 2022

Published: 28 January 2022

Publisher's Note: MDPI stays neutral with regard to jurisdictional claims in published maps and institutional affiliations.



Copyright: © 2022 by the authors. Licensee MDPI, Basel, Switzerland. This article is an open access article distributed under the terms and conditions of the Creative Commons Attribution (CC BY) license (<https://creativecommons.org/licenses/by/4.0/>).

1. Introduction

Microcapsule healing materials [1–5] have attracted increasing attention and have been widely researched, especially since the first-generation healing system reported by White et al. [6] This is mainly because the microcapsule healing materials can provide instant feedback to external signals from the outside [7–11], complete the healing automatically and significantly extend the service life [12–16]. As reported in previous work [17,18], healing reagents must be encapsulated in capsules before being added to self-healing coatings to offer the self-healing functions [19]. If the self-healing coating was cracked and damaged, the embedded microcapsules would release the healing reagents after rupture and refill the cracked area [20–25]. Thus, a microcapsule must possess several features, including suitable protective ability for the core material [26–28], excellent repair efficiency and high encapsulation efficiency [29,30]. Furthermore, for a microcapsule's application in the coating industry, the simplicity of its preparation process and mass production are also important [31–33].

Various methods of preparing self-healing microcapsules have already been widely reported. Yang et al. [34] prepared a kind of microcapsule with isophorone diisocyanate (IPDI) as the core material and polyurethane (PU) as the shell material by interfacial polymerization. They prepared smooth spherical microcapsules with a diameter of 40 to 400 µm by controlling the stirring rate, and found that the thickness of the shell material

changes linearly with the diameter of the microcapsule. Wang et al. [35] added IPDI-coated microcapsules to alkyd resin varnish (ACVS), and combined the scanning reference electrode method (SMRE) and FTIR to directly demonstrate the self-healing performance of the IPDI-ACVS system. Credico et al. [36] used double-layer polyurethane/polyurea formaldehyde polyurethane (PUF) as the shell material and IPDI as the core material to prepare the microcapsule with a regular surface. Then, they added the microcapsules to the resin matrix and made scratches on the surface of the material. After 48 h of repairing them in water, the scratches on the surface basically disappeared. Li et al. [37] used polyetheramine (PEA) as the core material and polymethyl methacrylate (PMMA) as the shell material to prepare a series of curing agent microcapsules by solvent evaporation. The microcapsules with different morphologies, shell wall thickness and particle size distribution were obtained by adjusting the reaction temperature, core to shell ratio, stirring speed, emulsifier concentration and other process conditions. Liang et al. [38] used IPDI as the core material and polysulfide network structure resin as the shell material, and prepared a new type of microcapsule through the method of interfacial polymerization.

However, previous studies have mainly focused on microcapsules where the core material comprised monomers such as IPDI [39]. Moreover, as the core material of microcapsules for self-healing coatings, IPDI, is unstable, the reaction products had poor elasticity and low toughness because of the lack of soft segments, which can easily cause secondary damage. These shortcomings severely limited the development of IPDI microcapsules, so it is necessary to develop a microcapsule material with high elasticity and a high toughness repair agent.

In this work, isocyanate prepolymer formed by isocyanate-terminated polyetheramine D2000 was used as the core material. Compared with IPDI monomer, isocyanate prepolymer as the healing agent can significantly increase the repair efficiency of microcapsules. In addition, it was different from the traditional microcapsule of monomer repair agents, the curing speed of the prepolymer healing agent was faster, there were many soft segment structures in the formed polyurea and the formed repair area had elasticity and toughness, which could reduce the probability of secondary damage. Furthermore, in the oil-in-water (O/W) system, Bayer L-75 and BDO were used to react the chain extension. The reaction process was controllable and significantly improved the reaction rate of the interfacial polymerization to form a membrane that could protect the core material from the water phase and reduce the loss of core material during the preparation of microcapsules. Additionally, the encapsulation efficiency was improved through the reaction process. Therefore, our research has important implications for improving the practicality of microcapsule self-healing materials [40].

2. Materials and Methods

2.1. Materials

Gum Arabic (GA, pharmaceutical grade), butyl acetate (BA, 99.5%), isophorone diisocyanate (IPDI, 99%) and polyetheramine D2000 (PEA, average $M_n \approx 2000$) were purchased from Shanghai Aladdin Biochemical Technology Co., Ltd., Shanghai, China. 1,4-butanediol (BDO, 99%) was purchased from Shanghai Maclean Biochemical Technology Co., Ltd. Shanghai, China. The commercial polyurethane curing agent Bayer L-75 was supplied by Shanghai Covestro Polymer Co., Ltd. Shanghai, China. The two-component epoxy resin AB glue (YT-CC302Q) was purchased from Kunshan Yituo Composite Material Co., Ltd. Kunshan, China. Deionized (DI) water in all experiments was purified with HHitech (Shanghai, China) purification equipment by deionization and filtration to a resistivity above 18.2 $M\Omega \cdot cm$.

2.2. Preparation of Isocyanate Prepolymer

The polyetheramine prepolymer was prepared by the one-step method. Isophorone diisocyanate (IPDI, 2.33 g) and butyl acetate (BA, 10 mL) were mixed in a three-necked flask and nitrogen gas was introduced to remove oxygen and moisture. Polyetheramine (PEA,

20 g) was injected into the three-necked flask dropwise with a syringe. The isocyanate prepolymer was obtained by reacting for 4 h at room temperature. The schematic diagram of prepolymer synthesis is shown in Figure 1.



Figure 1. Schematic diagram of synthesis of isocyanate prepolymer.

2.3. Preparation of Microcapsules

The microcapsules with different GA content and different BDO content were prepared according to the conditions of Table 1. A typical emulsion of sample MC2 was prepared by the following steps. First, the commercial polyurethane curing agent (Bayer L-75, 3 g) and polyetheramine D2000 prepolymer (PEA, 6 g) were dissolved in butyl acetate (BA, 2 mL) as the oil phase. Then, deionized water (DI, 37 mL) and gum Arabic (GA, 3 g) were added into a 100 mL beaker, and formed an emulsion under stirring. Next, the oil phase was quickly dropped into the emulsion and stirred at 600 rpm to form an oil-in-water system. 1,4-butanediol (BDO, 2 g) was added to the system dropwise within 3 min and we made sure the system was heated to 60 °C. After 3 h of reaction, a microcapsule suspension was obtained. Finally, the microcapsule sample was obtained after drying for 24 h.

Table 1. Recipes of the microcapsule synthesis with different GA and BDO concentrations.

Sample	m(GA)/g	m(L-75)/g	m(Isocyanate Prepolymer)/g	m(BDO)/g
MC1	2	3	6	2
MC2	3	3	6	2
MC3	5	3	6	2
MC4	3	3	6	2.5
MC5	3	3	6	1

2.4. Core Content Determination

In order to investigate the effect of emulsifier concentration on the encapsulation rate of microcapsules, the core content was calculated by the extraction method [41]. The proper amounts of microcapsules (M_0) were weighed and then crushed by pestle grinding in the presence of acetone as the extractant, then filtered and dried, and the remaining material (M_s) was weighed. The core content (W) could be calculated according to the following formula.

$$W(\%) = \frac{M_0 - M_s}{M_0} \times 100\% \quad (1)$$

2.5. Characterizations

Optical microscopy (OM): The morphology and particle size of microcapsule samples prepared with different emulsifier content and chain extender content were observed with BX53M OM of Olympus, Tokyo, Japan.

Scanning electron microscopy (SEM): The overall particle size and surface smoothness of microcapsules prepared with different emulsifier content and chain extender content were observed with a Japanese Hitachi SU8010 scanning electron microscope (Hitachi, Tokyo, Japan). operating at 5.0 kV.

Laser particle size analyzer: The particle size distribution of the prepared microcapsules was tested by the MS2000 laser particle size analyzer of Malvern, London, UK.

Fourier transform infrared spectra (FTIR): FTIR spectra of isocyanate prepolymer, microcapsules and their shell were performed with a Thermo Fisher Scientific NICOLET IS10 IR instrument (Thermo Fisher, Shanghai, China). The test range was from 400 to 4000 cm^{-1} .

X-ray diffraction (XRD): The crystal structure of the microcapsule was analyzed with the D8 ADVANCE XRD instrument from Bruker, Karlsruhe, Germany. The scanning range was from 10 to 80°, the working voltage was 40 kV and the current was 40 mA.

Thermal gravimetric analysis (TGA): TGA of isocyanate prepolymer, microcapsules and their shell were performed with a NETZSCH TAQ 2000 instrument (Netzsch, Shanghai, China). The typical experimental process of TGA was as follows: 3 to 6 mg samples were neatly placed on an aluminum oxide crucible and heated from 30 to 500 °C at a heating rate of 10 °C min^{-1} under nitrogen atmosphere.

2.6. Evaluation of Self-Healing Performance

The self-healing coatings were prepared by dispersing the synthetic microcapsules evenly into the epoxy resin AB component. The coating samples were frozen at -40 °C for 4 h. Artificial scratches were created on the coatings using scissors. The specimens after scratching were kept at room temperature for 24 h for the healing process. The OM images of the scratched regions were obtained to reflect the healing behavior of the coatings with different microcapsule contents.

2.7. Evaluation of Anti-Corrosion Performance

The epoxy resin paintings with different microcapsule contents were obtained by mixing epoxy resin A and B components in a mass ratio of 3:1, and the microcapsule samples with mass fractions of 10% and 20% were added to it. Then, according to the standard, two coatings with different capsule contents were applied to the pre-treated substrate, and cured at room temperature for 26 h. After the curing was completed, the coatings were scratched to study their anti-corrosion and healing conditions. The pure epoxy resin coating and 10% microcapsule content and 20% microcapsule content self-healing coatings were scratched with a blade, and we tried to give the cracks of each group the same width and depth. In order to speed up the corrosion rate and deepen the corrosion effect, the three coating samples were immersed in 3.5 wt% NaCl solution, and the corrosion of the coating cracks was observed and recorded every 24 h, with continuous observation and recording for 72 h.

3. Results and Discussion

As in the schematic plot shown in Figure 2a, O/W emulsion stabilized was prepared by gum Arabic (GA), and oil phase was the mixture of isocyanate prepolymer and Bayer L-75. Bayer L-75, an aromatic diisocyanate, was much more reactive than isocyanate prepolymer (aliphatic isocyanate) towards amines or alcoholic molecules. Thus, isocyanate groups of Bayer L-75 preemptively reacted with hydroxyls of BDO or water at the interface of emulsion droplets and formed a thin PU membrane. Then, microcapsules were formed by interfacial polymerization.

When the self-healing coating was cracked and damaged (Figure 2b), the embedded microcapsules would release the isocyanate prepolymer after rupture, and refilled the cracked area. When it encountered water in the matrix or in the air, the isocyanate prepolymer reacted with water to form an unstable carbamate, which would later decompose into amine and carbon dioxide. The amine group could further react with the isocyanate group to form a urea-containing polymer to repair the crack. The advantage of this work is that it reduces the possibility of secondary damage.

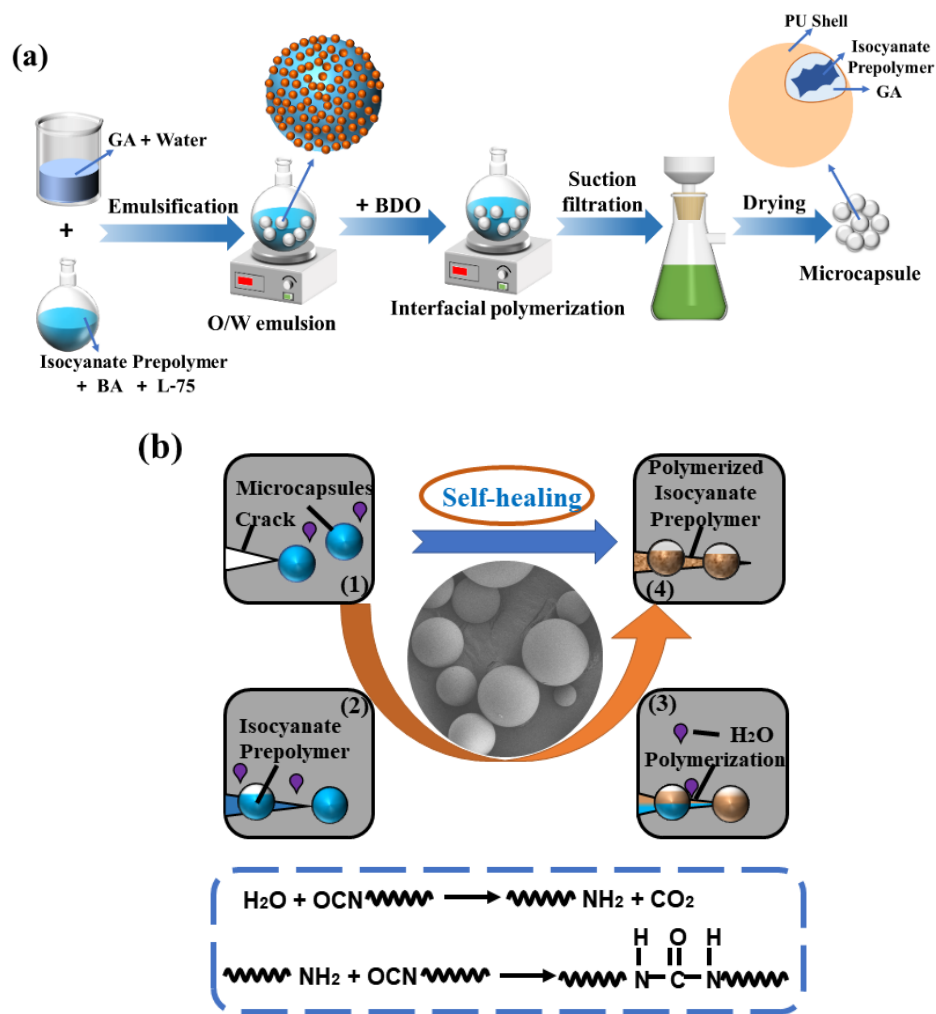


Figure 2. (a) Preparation path diagram of microcapsules. (b) Mechanism diagram of the self-healing of isocyanate prepolymer microcapsules.

3.1. Analysis of the Chemical Structure of Microcapsules

FTIR spectra of isocyanate prepolymer, the microcapsules and their shell were conducted to further reveal the chemical structure of the microcapsules (Figure 3a). From Figure 3a, it can be seen that they all have a characteristic peak at 3320 cm^{-1} ; in addition, the microcapsules and isocyanate prepolymer have an absorption peak at 2254 cm^{-1} . With wide stretching vibration peaks of N-H at about 3320 cm^{-1} , stretching vibration peaks of aliphatic C=O at 1713 cm^{-1} existed in the spectrum of the microcapsules and their shell, which proved that the microcapsules had urethane groups (-NHCOO) and successfully formed the polyurethane shell material.

Stretching vibration peaks of isocyanate groups (-NCO) at about 2254 cm^{-1} existed in the spectrum of microcapsules and isocyanate prepolymer because the isocyanate prepolymer was blocked by isocyanate. The absorption peak at 2254 cm^{-1} proved that the isocyanate prepolymer was successfully synthesized. The stretching vibration peak of C=O at 1713 cm^{-1} belonged to the urea group synthesized by the reaction of PEA D2000 and isocyanate, proving the successful polymerization of isocyanate and amine. Because several microcapsules were broken and a small amount of prepolymer flowed out, the characteristic peaks of isocyanate groups also appeared in the infrared spectrum of the microcapsules, which proved that the core material isocyanate prepolymer was efficiently encapsulated in the isocyanate prepolymer microcapsules as a healing agent.

In order to verify the successful synthesis of the polyurethane shell, X-ray diffraction tests were performed on the microcapsules and their shell (Figure 3b). As shown in

Figure 3b, there was a larger amorphous peak at $2\theta = 20^\circ$, which was the XRD characteristic peak of polyurethane, proving that the outer shell of the microcapsule was made of polyurethane.

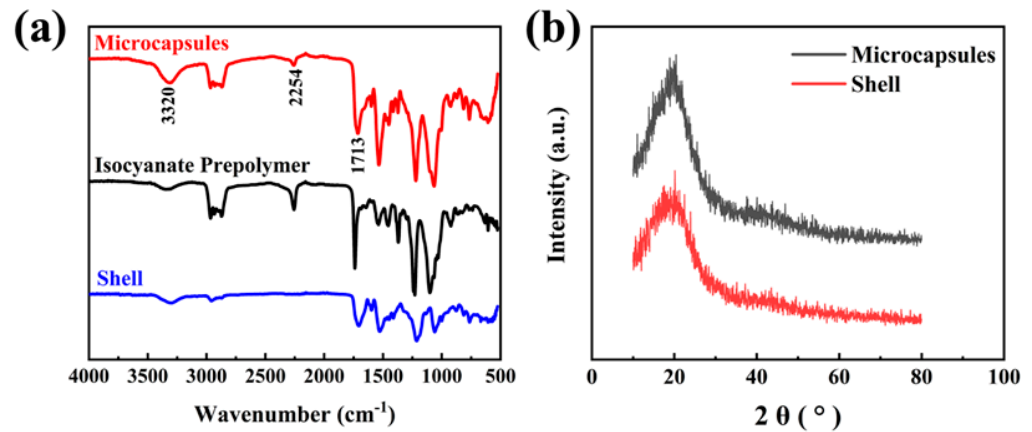


Figure 3. (a) FTIR spectra of isocyanate prepolymer, shell and microcapsules. (b) XRD diagram of microcapsules.

3.2. Effect of the Concentration of Gum Arabic on Microcapsules

In the process of emulsifying the oil phase, the concentration of the emulsifier had a notable influence on the stability of the emulsion, and further affected the morphology, particle size and distribution of the final microcapsules. Therefore, the influence of the amount of gum Arabic (GA) on the surface morphology of the microcapsule was investigated. The microcapsules with different GA dosages were prepared according to the conditions of Table 1.

Figure 4 contains the OM and SEM images of the microcapsules with different GA dosages. The concentrations of the emulsifier in the microcapsule samples in Figure 4a–c are 5%, 7.5% and 12.5%, respectively. It can be seen from the figures that when the amount of emulsifier was 5%, the microcapsules were not uniform in particle size and a small amount of microcapsules ruptured; this may be due to the low concentration of GA, which could not form a sufficient oil-in-water (O/W) system. As the concentration of GA increased to 7.5%, the sphericity of the prepolymer microcapsules became higher and higher, the particle size increased gradually, the particle size became uniform and there was no rupture, because the surface tension of the water phase gradually decreases with the increase in GA mass fraction in the early stage and the stability of the two-phase interface was strengthened. Thus, the microcapsules formed have higher strength and less breakage. When the concentration of emulsifier was further increased to 12.5%, the particle size of microcapsules became smaller again, because when the amount of emulsifier significantly increases, the water–oil interface gathers many emulsifier molecules and needs to provide more. In addition, the viscosity of the system increased with the increase in GA mass fraction. It was not only difficult to stir, but also in the process of stirring, small droplets were likely to collide and combine into large droplets, and large droplets were more likely to break when they collided, so the microcapsule rupture phenomenon would increase significantly. The concentration of emulsifier GA in this experiment was controlled at 7.5%, and the prepared microcapsules had a smooth surface, complete morphology, suitable particle size and uniform distribution.

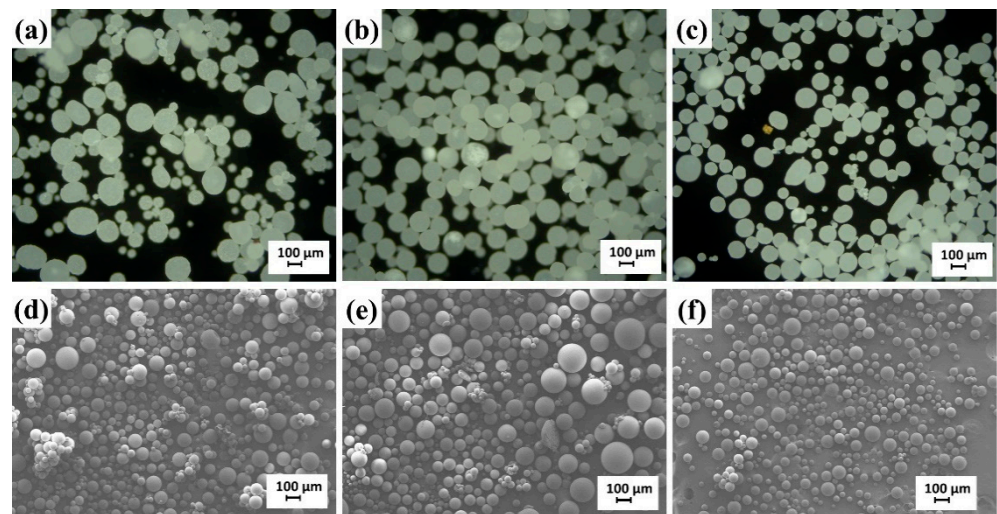


Figure 4. OM and SEM images of the microcapsules with different GA dosages: (a) 5 wt%, (b) 7.5 wt%, (c) 12.5 wt%, (d) 5 wt%, (e) 7.5 wt%, (f) 12.5 wt%.

3.3. Effect of the Concentration of BDO on Microcapsules

The OM and SEM images of the microcapsules with different BDO contents are shown in Figure 5. The mass concentrations of BDO in Figure 5a–c are 8.33%, 15.38% and 18.52% (relative to the mass fraction of the core and shell material), respectively. The size of the microcapsule increased with the increase in the concentration of BDO. The particle size of the microcapsules was small when the mass fraction of BDO was 8.33%, which could be because the BDO content was insufficient at this time and could not effectively act as a chain extender, and there were many isocyanate groups in the raw materials that reacted with the hydroxyl group (-OH) of water, resulting in a lower content of synthetic shell materials and a smaller particle size of the microcapsules. As the BDO mass fraction increased to 15.38%, the particle size of the microcapsule increased and the distribution was also uniform, but the distribution became uneven when it increased to 18.52%. This may be because as the mass fraction of BDO increased, more microcapsules were involved in chain extension, and the diameter of the microcapsules further increased. When the mass fraction of BDO was higher, the reaction rate of the hydroxyl group and the isocyanate group significantly increased, making it difficult to keep the reaction rate of the entire system stable. As a result, the particle size of the synthesized microcapsules varied greatly. In summary, when the mass fraction of BDO was about 15.38%, the prepared microcapsules had a uniform particle size, and the average particle size of microcapsules was 124.39 μm , which was relatively moderate.

3.4. Core Content

The core content of the microcapsule has a greater impact on its repair efficiency, so we calculated the core content according to Formula (1). The core contents of the prepared microcapsule samples were 31.56%, 40.88% and 32.13% when the GA concentrations were 5 wt%, 7.5 wt% and 12.5 wt%, respectively. This was because the emulsifier increased the stability of the emulsion, and more emulsion films coated the surface of the oil droplets, so the core content of the microcapsules increased. However, when the concentration of emulsifier increased to 12.5 wt%, the emulsion formed was too viscous, so not only was it more difficult to disperse the emulsion, but the emulsion film on the surface of the oil droplets was also very thick, and it was difficult to deposit the synthetic wall material onto the surface of the oil droplets; thus, it was hard to effectively encapsulate the core material.

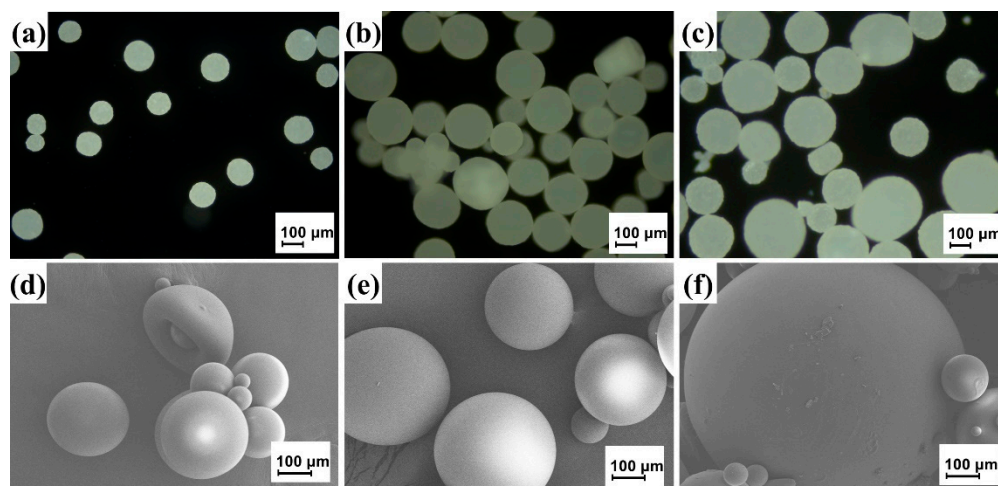


Figure 5. (a–c) OM images of the microcapsules with different BDO dosages. (d,e) SEM images of the microcapsules with different BDO dosages. (a,d) 8.33 wt%, (b,e) 15.38 wt%, (c,f) 18.52 wt%.

3.5. Particle Size and Thermal Analysis of Microcapsules

Figure 6a shows the particle size distribution of sample MC1 to MC5. As shown in Figure 6a, the particle size of the microcapsules increased with the increase in the concentration of GA from 5% to 7.5%. When the mass fraction of GA was 7.5%, the particle size of the microcapsules was moderate and the distribution was concentrated, mostly from 50 to 240 μm, with an average particle size of about 124.39 μm. As the mass fraction continued increasing, the overall particle size gradually decreased and the distribution was uneven, and the span of the particle size distribution was slightly larger, consistent with the OM and SEM images in Figure 4. This could be explained by the fact that the likelihood of merging between droplets decreased and the particle size decreased with the increase in the amount of emulsifier. Moreover, in the process of synthesizing microcapsules, smaller microcapsules were formed near the stirring rotor, and larger microcapsules were far away from the stirring rotor, resulting in a wider size distribution of microcapsules.

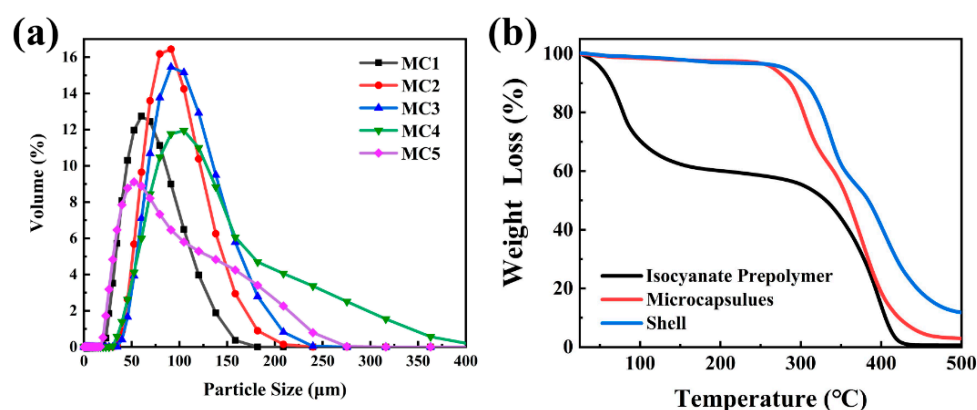


Figure 6. (a) Particle size distribution of microcapsules. (b) TGA curves of isocyanate prepolymer, microcapsules and shell.

When the concentration of BDO was 8.33%, the particle size of the microcapsules was small. This was because BDO had a small mass fraction and low content relative to the core wall and could not effectively function as a chain extender. There were many isocyanate groups in the raw materials. The group (-NCO) reacted with the hydroxyl group (-OH) of water, resulting in less wall material content, so the particle size of the microcapsules was smaller. When the mass fraction of BDO increased to 15.38 wt%, the particle size of the microcapsules also increased, but when the relative core wall mass fraction of BDO increased to 18.52 wt%, the particle size of the microcapsules increased, but the particle size distribution was uneven. This is because when the mass fraction of BDO was high, the reaction rate of -OH and -NCO significantly increased, making it difficult to keep the reaction rate of the whole system stable, and the size of the synthesized microcapsules varied greatly.

As a container for active self-healing reagents, the thermal stability of microcapsules is important for their practical applications. Therefore, TGA tests were performed on the core material isocyanate prepolymer, the polyurethane shell and the microcapsules (Figure 6b).

As shown in Figure 6b, isocyanate prepolymer lost 5% weight at 65 °C because of the continuous evaporation of butyl acetate in the isocyanate prepolymer solution during the heating process, while the microcapsules had a little thermal decomposition from 30 to 270 °C. This may be because a few microcapsules were damaged during preparation, and the isocyanate prepolymer was thermally decomposed at this temperature. Thus, we confirmed that the core material had improved heat resistance under the urethane shell. The TGA curves also showed that the weight loss of microcapsules was mainly divided into two stages. The first stage occurred in the temperature range of about 270 to 330 °C, which could be attributed to the thermal decomposition of the polyurethane shell and the evaporation of the solvent. The second stage occurred in the temperature range of about 330 to 430 °C, which was attributed to the homopolymerization reaction of the encapsulating resin.

Due to the high viscosity of the shell material, it was difficult to prepare and sample it separately; therefore, the shell material was prepared without adding isocyanate prepolymer in the reaction system. The method was the same as for preparing the microcapsules, and we only obtained the microcapsule sample containing the shell material. As shown in Figure 6b, the quality of the polyurethane shell material remained stable from 30 to 270 °C and the TGA curve of the shell material began to drop sharply until 290 °C, at which point the decomposition temperature of the shell material was reached. We also observed that the mass fraction of the shell did not change after 470 °C because the shell material decomposed and the remaining material was the residue after carbonization.

3.6. Preliminary Self-Healing and Anti-Corrosion Performance of Epoxy Coatings

Epoxy resins are widely used in coatings because of their excellent chemical resistance, strong paint film adhesion and excellent anti-corrosion properties. Therefore, we added microcapsules to epoxy resin adhesive to develop healing coatings. The repair mechanism of the self-healing coating is shown in Figure 2b. Self-healing epoxy coatings were prepared using epoxy resin AB glue by adding synthetic microcapsules with different weight ratios, i.e., 0 wt%, 10 wt% and 20 wt% of MC2. Figure 7 shows the OM images of cracked planes after healing in coatings with (a) 0 wt% MC2, (b) 10 wt% MC2 and (c) 20 wt% MC2. The OM image shows that the cracks applied in the epoxy coating with 10 wt% or 20 wt% MC2 were slightly filled. It illustrates that the microcapsules dispersed in the epoxy resin matrix had a healing effect. Similarly, the Figure 7b for the coating with 10 wt% MC2 shown better self-healing, as the width and depth of the crack reduced significantly. Therefore, the epoxy resin AB glue coating with 10 wt% MC2 had the strongest self-healing capability.

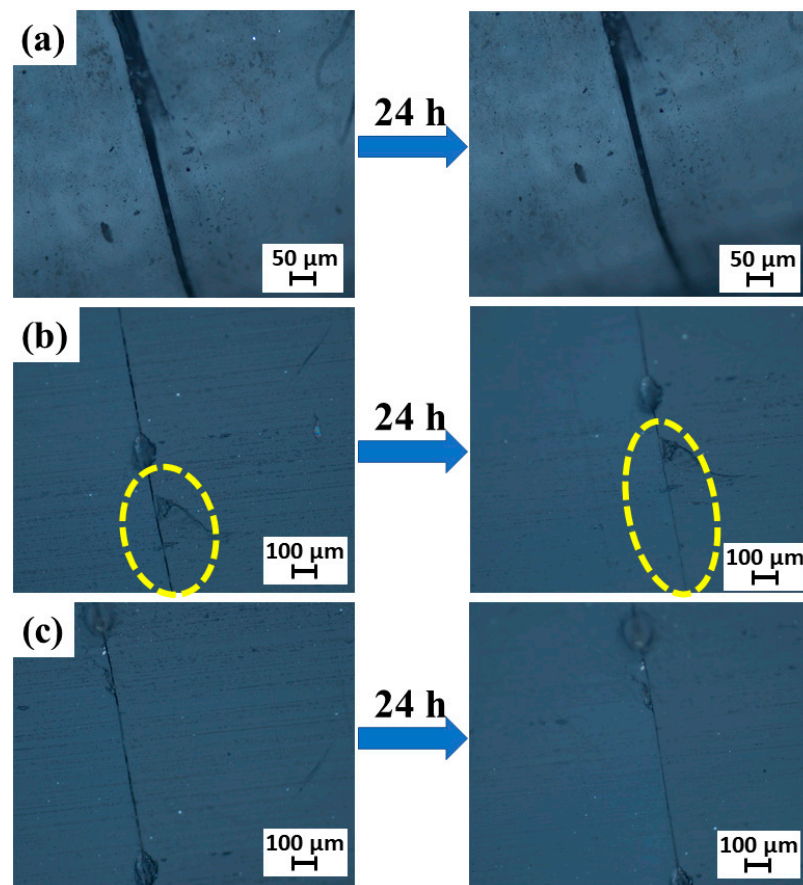


Figure 7. Images of a cracked plane after healing with epoxy coatings with (a) 0 wt% MC2, (b) 10 wt% MC2 and (c) 20 wt% MC2.

In order to observe the corrosion in a short period of time, the coatings were scratched and then immersed in NaCl solution. The three groups of coating specimens were immersed in 3.5 wt% NaCl solution, and the corrosion at the cracks of the coating was observed and photographed and recorded every 24 h for 72 h. The results are shown in Figure 8.

It can be seen from Figure 8 that the coating samples immersed in NaCl solution showed no obvious corrosion, except for the scratched area without microcapsule coating. This is because the scratches lost the protection of the original coating and were in direct contact with the NaCl solution, thereby being corroded. After adding the microcapsules, the scratch would puncture the microcapsules, causing the core repair agents to be released and flow to the crack, where they reacted with water to form a polymer that repaired the scratch area. Therefore, they effectively protected the substrate and enhanced the corrosion resistance of the coating. In addition, the scratch area of the coating samples with 10% and 20% microcapsules content was reduced after being dipped into NaCl solution, and the scratches became shallower and lighter. The coating with 20% microcapsule content showed some blistering and flaking after 72 h of immersion because adding too many microcapsules changed the original performance of the coating, resulting in the adhesion of the coating decreasing and blistering the coating with a long immersion time. Comprehensive analysis, taking into account the corrosion and adhesion of the coating, should incorporate the epoxy resin coating ratio of about 10% of the prepolymer microcapsules.

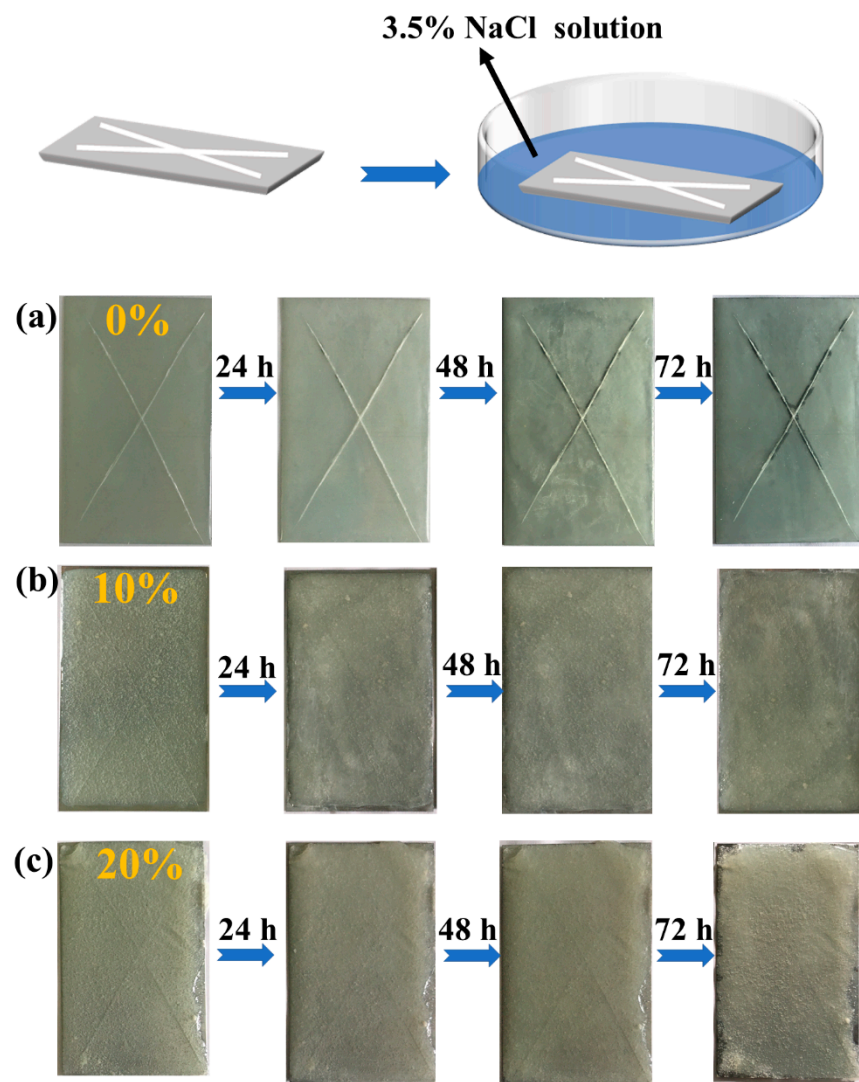


Figure 8. Corrosion of three groups of coatings with different microcapsule content after soaking in NaCl solution. (a) 0 wt% MC3, (b) 10 wt% MC3 and (c) 20 wt% MC3.

4. Conclusions

Isocyanate prepolymer microcapsules, richly loaded with isocyanate group-terminated polyetheramine, were synthesized by interfacial polymerization. The size control of microcapsules was deftly conducted by varying the GA contents and BDO contents. The addition of GA was beneficial to reduce the adhesion phenomenon and enhance the smoothness of the microcapsule surface. The addition of BDO was beneficial to the formation of microcapsules and the enlargement of the particle size. Our research shows that the microcapsules were in a regular spherical shape with a smooth surface and a moderate particle size when the concentration of GA was 7.5% and the mass fraction of BDO was 15.38%. The mean diameter scale of the capsules was about 50 to 240 μm , the average particle size was about 124.39 μm and the core content of the microcapsule sample was 40.88%. Furthermore, due to the protective effect of the polyurethane shell, the microcapsules also showed thermal stability at 270 $^{\circ}\text{C}$. These favorable properties of isocyanate prepolymer microcapsules provide strong support for their further application in industrial fields. The self-healing test of the coating showed that when microcracks appeared inside the coating, the isocyanate prepolymer microcapsules also ruptured, releasing the isocyanate prepolymer, which reacted with water to produce polymer, thus filling the cracks and achieving the effect of self-healing. The corrosion resistance analysis of the coating showed that the blank coating specimens without microcapsules were seriously corroded at the cracks after soaking in

NaCl solution for 72 h, while the self-healing coating with prepolymer microcapsules was not corroded at the cracks after soaking.

Author Contributions: Conceptualization, G.X. and X.G.; methodology, G.X. and J.T. (Jing Tu); software, H.X.; validation, J.J., H.L. and L.L.; formal analysis, G.X.; investigation, J.J.; resources, G.X.; data curation, G.X.; writing—original draft preparation, G.X.; writing—review and editing, G.X.; visualization, G.X. and H.C.; supervision, G.X. and J.T. (Jingqing Tian); project administration, G.X.; funding acquisition, X.G. All authors have read and agreed to the published version of the manuscript.

Funding: The authors thank the financial support for the Graduate Research and Innovation Program of Jiangsu province (Grant No. KYCX21_0288). And this work was supported by the equipment support from the Analysis and Testing Center of Nanjing University of Science and Technology and the analysis support from Shiyanjia Lab (www.shiyanjia.com, accessed on 22 December 2021).

Institutional Review Board Statement: Not applicable.

Informed Consent Statement: Not applicable.

Data Availability Statement: Data sharing not applicable.

Conflicts of Interest: The authors declare no conflict of interest.

References

1. Wilson, G.O.; Moore, J.S.; White, S.R.; Sottos, N.R.; Andersson, H.M. Autonomic healing of epoxy vinyl esters via ring opening metathesis polymerization. *Adv. Funct. Mater.* **2008**, *18*, 44–52. [[CrossRef](#)]
2. Jin, H.; Mangun, C.L.; Stradley, D.S.; Moore, J.S.; Sottos, N.R.; White, S.R. Self-healing thermoset using encapsulated epoxy-amine healing chemistry. *Polymer* **2012**, *53*, 581–587. [[CrossRef](#)]
3. Zhu, D.Y.; Wetzel, B.; Noll, A.; Rong, M.Z.; Zhang, M.Q. Thermo-molded self-healing thermoplastics containing multilayer microreactors. *J. Mater. Chem. A* **2013**, *1*, 7191–7198. [[CrossRef](#)]
4. Jin, H.; Mangun, C.L.; Griffin, A.S.; Moore, J.S.; Sottos, N.R.; White, S.R. Thermally stable autonomic healing in epoxy using a dual-microcapsule system. *Adv. Mater.* **2014**, *26*, 282–287. [[CrossRef](#)] [[PubMed](#)]
5. Teixeira, R.F.A.; van den Berg, O.; Nguyen, L.T.T.; Fehér, K.; Du Prez, F.E. Microencapsulation of active ingredients using PDMS as shell material. *Macromolecules* **2014**, *47*, 8231–8237. [[CrossRef](#)]
6. White, S.R.; Sottos, N.R.; Geubelle, P.H.; Moore, J.S.; Kessler, M.R.; Sriram, S.R.; Brown, E.N.; Viswanathan, S. Autonomic healing of polymer composites. *Nature* **2001**, *409*, 794–797. [[CrossRef](#)]
7. Alizadegan, F.; Mirabedini, S.M.; Pazokifard, S.; Moghadam, S.G.; Farnood, R. Improving self-healing performance of polyurethane coatings using PU microcapsules containing bulky-IPDI-BA and nano-clay. *Prog. Org. Coat.* **2018**, *123*, 350–361. [[CrossRef](#)]
8. Cao, C.F.; Liu, W.J.; Xu, H.; Yu, K.X.; Gong, L.X.; Guo, B.F.; Li, Y.T.; Feng, X.L.; Lv, L.Y.; Pan, H.T.; et al. Temperature-induced resistance transition behaviors of melamine sponge composites wrapped with different graphene oxide derivatives. *J. Mater. Sci. Technol.* **2021**, *85*, 194–204. [[CrossRef](#)]
9. Cao, B.; Souza, L.; Xu, J.; Mao, W.; Wang, F.; Al-Tabbaa, A. Soil mix cutoff wall materials with microcapsule-based self-Healing grout. *J. Geotech. Geoenviron. Eng.* **2021**, *147*, 04021124. [[CrossRef](#)]
10. Nguyen, L.T.T.; Hillewaere, X.K.D.; Teixeira, R.F.A.; van den Berg, O.; Du Prez, F.E. Efficient microencapsulation of a liquid isocyanate with in situ shell functionalization. *Polym. Chem.* **2015**, *6*, 1159–1170. [[CrossRef](#)]
11. Song, Y.; Chen, K.F.; Wang, J.J.; Liu, Y.; Qi, T.; Li, G.L. Synthesis of polyurethane/poly (urea-formaldehyde) double-shelled microcapsules for self-healing anticorrosion coatings. *Chin. J. Polym. Sci.* **2020**, *38*, 45–52. [[CrossRef](#)]
12. Jeoung, H.J.; Kim, K.W.; Chang, Y.J.; Jung, Y.C.; Ku, H.; Oh, K.W.; Choi, H.M.; Chung, J.W. Self-healing EPDM rubbers with highly stable and mechanically-enhanced urea-formaldehyde (UF) microcapsules prepared by multi-step in situ polymerization. *Polymers* **2020**, *12*, 1918. [[CrossRef](#)]
13. Rodriguez, R.; Bekas, D.G.; Flórez, S.; Kosarli, M.; Paipetis, A.S. Development of self-contained microcapsules for optimised catalyst position in self-healing materials. *Polymer* **2020**, *187*, 122084. [[CrossRef](#)]
14. Fan, W.; Zhang, Y.; Li, W.; Wang, W.; Zhao, X.; Song, L. Multilevel self-healing ability of shape memory polyurethane coating with microcapsules by induction heating. *Chem. Eng. J.* **2019**, *368*, 1033–1044. [[CrossRef](#)]
15. Chen, L.; Yu, H.; Li, W.; Dirican, M.; Liu, Y.; Zhang, X. Interlayer design based on carbon materials for lithium–sulfur batteries: A review. *J. Mater. Chem. A* **2020**, *8*, 10709–10735. [[CrossRef](#)]
16. Zhou, S.; Jia, Y.; Wang, C. Global sensitivity analysis for the polymeric microcapsules in self-healing cementitious composites. *Polymers* **2020**, *12*, 2990. [[CrossRef](#)]
17. Shchukin, D.G. Container-based multifunctional self-healing polymer coatings. *Polym. Chem.* **2013**, *4*, 4871–4877. [[CrossRef](#)]
18. Blaiszik, B.J.; Jones, A.R.; Sottos, N.R.; White, S.R. Microencapsulation of gallium–indium (Ga–In) liquid metal for self-healing applications. *J. Microencapsul.* **2014**, *31*, 350–354. [[CrossRef](#)]

19. Wu, G.; An, J.; Sun, D.; Tang, X.; Xiang, Y.; Yang, J. Robust microcapsules with polyurea/silica hybrid shell for one-part self-healing anticorrosion coatings. *J. Mater. Chem. A* **2014**, *2*, 11614–11620. [[CrossRef](#)]
20. Habib, S.; Khan, A.; Nawaz, M.; Sliem, M.H.R.; Shakoor, R.A.; Kahraman, R.; Abdullah, A.M.; Zekri, A. Self-healing performance of multifunctional polymeric smart coatings. *Polymers* **2019**, *11*, 1519. [[CrossRef](#)]
21. An, S.; Yoon, S.S.; Lee, M.W. Self-healing structural materials. *Polymers* **2021**, *13*, 2297. [[CrossRef](#)]
22. Yan, X.; Peng, W. Preparation of microcapsules of urea formaldehyde resin coated waterborne coatings and their effect on properties of wood crackle coating. *Coatings* **2020**, *10*, 764. [[CrossRef](#)]
23. Tao, Z.; Cui, J.; Qiu, H.; Yang, J.; Gao, S.; Li, J. Microcapsule/silica dual-fillers for self-healing, self-reporting and corrosion protection properties of waterborne epoxy coatings. *Prog. Org. Coat.* **2021**, *159*, 106394. [[CrossRef](#)]
24. Katouezadeh, E.; Zebarjad, S.M.; Janghorban, K. Mechanical properties of epoxy composites embedded with functionalized urea-formaldehyde microcapsules containing an oxidizable oil. *Mater. Chem. Phys.* **2021**, *260*, 124106. [[CrossRef](#)]
25. Attaei, M.; Loureiro, M.V.; Do Vale, M.; Condeço, J.A.; Pinho, I.; Bordado, J.C.; Marques, A.C. Isophorone diisocyanate (IPDI) microencapsulation for mono-component adhesives: Effect of the active H and NCO sources. *Polymers* **2018**, *10*, 825. [[CrossRef](#)] [[PubMed](#)]
26. Attaei, M.; Calado, L.M.; Taryba, M.G.; Morozov, Y.; Shakoor, R.A.; Kahramna, R.; Marques, A.C.; Monmor, M.F. Autonomous self-healing in epoxy coatings provided by high efficiency isophorone diisocyanate (IPDI) microcapsules for protection of carbon steel. *Prog. Org. Coat.* **2020**, *139*, 105445. [[CrossRef](#)]
27. Fathabadi, H.F.; Javidi, M. Self-Healing and Corrosion Performance of Polyurethane Coating Containing Polyurethane Microcapsules. Preprint. 2021. Available online: <https://doi.org/10.21203/rs.3.rs-348120/v1> (accessed on 30 March 2021).
28. Haghayegh, M.; Mirabedini, S.M.; Yeganeh, H. Preparation of microcapsules containing multi-functional reactive isocyanate-terminated-polyurethane-prepolymer as healing agent, part II: Corrosion performance and mechanical properties of a self-healing coating. *RSC Adv.* **2016**, *6*, 50874–50886. [[CrossRef](#)]
29. Nik Md Noordin Kahar, N.N.F.; Osman, A.F.; Alosime, E.; Arsat, N.; Azman, N.A.M.; Syamsir, A.; Itam, Z.; Hamid, Z.A.A. The versatility of polymeric materials as self-healing agents for various types of applications: A review. *Polymers* **2021**, *13*, 1194. [[CrossRef](#)]
30. Koh, E.; Kim, N.K.; Shin, J.; Kim, Y.W. Polyurethane microcapsules for self-healing paint coatings. *RSC Adv.* **2014**, *4*, 16214–16223. [[CrossRef](#)]
31. Dry, C. Procedures developed for self-repair of polymer matrix composite materials. *Compos. Struct.* **1996**, *35*, 263–269. [[CrossRef](#)]
32. Li, J.; Shi, H.; Liu, F.; Han, E.H. Self-healing epoxy coating based on tung oil-containing microcapsules for corrosion protection. *Prog. Org. Coat.* **2021**, *156*, 106236. [[CrossRef](#)]
33. Sima, W.X.; Shao, Q.Q.; Sun, P.T.; Liang, C.; Yang, M.; Yin, Z.; Deng, Q. Magnetically gradient-distributed microcapsule/epoxy composites: Low capsule load and highly targeted self-healing performance. *Chem. Eng. J.* **2021**, *405*, 126908. [[CrossRef](#)]
34. Yang, J.; Keller, M.W.; Moore, J.S.; White, S.R.; Sottos, N.R. Microencapsulation of isocyanates for self-healing polymers. *Macromolecules* **2008**, *41*, 9650–9655. [[CrossRef](#)]
35. Wang, W.; Xu, L.; Li, X.; Lin, Z.; Yang, Y.; An, E. Self-healing mechanisms of water triggered smart coating in seawater. *J. Mater. Chem. A* **2014**, *2*, 1914–1921. [[CrossRef](#)]
36. Di Credico, B.; Levi, M.; Turri, S. An efficient method for the output of new self-repairing materials through a reactive isocyanate encapsulation. *Eur. Polym. J.* **2013**, *49*, 2467–2476. [[CrossRef](#)]
37. Woo, J.H.; Kim, N.H.; Kim, S.I.; Park, O.K.; Lee, J.H. Effects of the addition of boric acid on the physical properties of mx-ene/polyvinyl alcohol (PVA) nanocomposite. *Compos. Part B Eng.* **2020**, *199*, 108205. [[CrossRef](#)]
38. Liang, F.; Chen, W.; Ma, A.; Zhou, H.W.; Jin, X.L. Preparation and properties of isocyanate microcapsules by interfacial polymerization method. *Polym. Mater. Sci. Eng.* **2018**, *34*, 150–154
39. Yi, H.; Yang, Y.; Gu, X.; Huang, J.; Wang, C. Multilayer composite microcapsules synthesized by Pickering emulsion templates and their application in self-healing coating. *J. Mater. Chem. A* **2015**, *3*, 13749–13757. [[CrossRef](#)]
40. Santos, A.N.B.; Santos, D.J.; Carastan, D.J. Microencapsulation of reactive isocyanates for application in self-healing materials: A review. *J. Microencapsul.* **2021**, *38*, 338–356. [[CrossRef](#)]
41. Tripathi, M.; Dwivedi, R.; Kumar, D.; Roy, P.K. Thermal activation of mendable epoxy through inclusion of microcapsules and imidazole complexes. *Polym. Plast. Technol. Eng.* **2016**, *55*, 129–137. [[CrossRef](#)]